Materials Advances

ROYAL SOCIETY OF CHEMISTRY

PAPER

View Article Online
View Journal

Cite this: DOI: 10.1039/d6ma00342g

Templated synthesis of a Zr-formate zeolite - like metal organic framework

Laoura K. Komodiki, [a] Nikos Panagiotou, *[a] Giannis S. Papaefstathiou [b] and Anastasios J. Tasiopoulos *[a]

Received 11th March 2026,
Accepted 10th June 2026

DOI: 10.1039/d6ma00342g

rsc.li/materials-advances

The templated synthesis of a new 3-dimensional Zr-formate MOF with the formula **{[$Zr_6(\mu_3\text{-}O)_4(\mu_3\text{-}OH)_4(HCOO)_{12}]_3(Me_2NH_2)_6(4\text{-}MepyH)_6(Cl)_8(CoCl_4)_2$}$_n$** – **ZrFA-4** displaying a sodalite topology is reported. The assembly of the hexanuclear Zr secondary building unit of **ZrFA-4** to form the sodalite cage led to a giant $[Zr_6]_{24}$ capsule templated by organic and inorganic ions, including $[CoCl_4]^{2-}$, Cl^-, $Me_2NH_2^+$, and 4-$MepyH^+$. These $[Zr_6]_{24}$ capsules are connected through *anti–anti* bridging formate groups, giving rise to a 3-dimensional network. **ZrFA-4** represents the third example of a **sod** Zr-MOF and of zeolite-like Zr-MOF, in general, and the first example of a 3-dimensional Zr MOF made only with formate organic ligands. Its isolation highlights the structure-directing capability of the template molecules, which enabled the formation of a MOF based on the simplest carboxylate ligand (formate) with a topology that could only be achieved previously by designed synthesis using organic ligands with appropriate geometrical characteristics. **ZrFA-4** is stable in common organic solvents and displays a BET surface area of 262 $m^2\ g^{-1}$.

Introduction

Metal–organic frameworks (MOFs) have attracted a tremendous amount of research interest. This stems from their chemical, structural and topological variability that leads to an unlimited number of structures with varying network topologies, metal ions or secondary building units (SBUs), organic ligands, functional groups, etc[1–4] and their interesting properties that lead to applications[5,6] in areas such as gas storage/separation,[7–12] catalysis,[13–15] sensing[16–21] and removal of pollutants from the environment.[22–27] As a result, MOFs exhibiting the desirable structural characteristics for targeted applications can be designed. A key property required for the use of MOFs in real – world applications is their stability in air and aqueous media under a variety of conditions, including extreme ones such as very high or low pH values.[28] One well-known highly stable MOF is UiO-66 exhibiting a 12-coordinated hexanuclear $[Zr_6(\mu_3\text{-}O^{2-})_4(\mu_3\text{-}OH^-)_4(COO^-)_{12}]$-SBU ($[Zr_6]$-SBU).[29] Since the discovery of UiO-66-67-68, many more Zr-MOFs based on the hexanuclear Zr^{4+} cluster have been synthesized and used in several applications due to their increased chemical stability, although the latter occurs mainly under acidic conditions.[28,30,31] The simplest ones among the Zr-based MOFs synthesized were those containing only formate organic ligands. In fact, there are three Zr-formate complexes reported in the literature based on the $[Zr_6]$-SBU, **ZrFA**,[32,33] **ZF-2**[34] and **ZF-3**,[34,35] two of which can be categorized as MOFs since compound **ZF-2** is rather a high nuclearity oligomeric $[Zr_6]_6$ metal cluster (0-D compound).[34] These compounds were synthesized by employing one or more additives in the reaction mixture, highlighting their important role in the stabilization of new MOF structures. In general, the synthesis of functional MOFs depends on many parameters such as starting Zr^{IV} source, ligand's characteristics such as donor groups, size, geometry and flexibility, synthesis solvents, the modulator used, reaction temperature and time as well as the presence in the reaction mixture of various additives.[36–38] The effect of the additives in the formation of new MOF structures has been systematically studied by several groups, including ours.[39–43] For example, in previous studies, we had investigated the role of aminoalcohols in reactions of Zn salts with a very common tricarboxylic ligand, trimesic acid[39] and extended this work to other polycarboxylic ligands such as pyridine-3,5-dicarboxylic acid and various amino- or pyridine-based alcohols as templates in the presence of different bipositive d-metal ions.[40] This approach led to the isolation of several new coordination polymers and MOFs with diverse dimensionalities (0D to 3D) and, in certain cases, previously unreported topologies.[44] The additive molecules were found to influence the structure and dimensionality of the resulting frameworks by acting as hydrogen-bond donors, space-filling agents, or chelating ligands, highlighting their critical role in directing framework assembly. The use of such structure-directing reaction parameters leads to a variety of MOFs with

[a] Department of Chemistry, University of Cyprus, 1678 Nicosia, Cyprus. E-mail: atasio@ucy.ac.cy, npanag06@ucy.ac.cy
[b] Laboratory of Inorganic Chemistry, Department of Chemistry, National and Kapodistrian University of Athens, Panepistimiopolis, Zografou 157 71, Greece

different network topologies and functionalities, and usually increases the elements of serendipity in reactions targeting functional MOFs.[45,46] On the other hand, there are strategies that are based mainly on the designed synthesis of MOFs with specific structural features that can lead to targeted properties. One well – known method employed for the rational synthesis of selected MOFs is the molecular building block (MBB) approach, which involves the connection of given SBUs using appropriate linkers, leading to new compounds possessing the targeted structural features.[47]

In particular, in the family of Zr – MOFs, the connectivity and structural characteristics of the [Zr_6]-SBU are mainly controlled by the donor groups and geometry of the linker or the type of the modulator used in the reaction mixture.[36,48] For example, the use of N/O donor ligands allowed the designed synthesis of heterometallic Zr/M′-MOFs (M′: transition metal ions or lanthanide ions).[49–51] Consequently, numerous strategies for synthesizing heterometallic MOFs were developed[49,50] leading to a series of functional materials[52,53] with multiple potential applications in CO_2 reduction,[54,55] H_2O oxidation,[55] magnetism,[56,57] temperature sensing,[58] H_2S removal[59] and solar cell platforms.[60] Another elegant example of designed synthesis targeting the formation of zeolitic-zirconium based MOFs, was provided by Eddaoudi and co-workers, who employed a cantellation strategy to induce the formation of 12-c Zr-**sod**-ZMOFs-1 and -2. This strategy involved the meticulous design of sterically hindered dicarboxylic ligands to avoid the formation of **dia** networks.[61] Even though Zr-MOFs have attracted a tremendous research interest and MOFs with the **sod** (and zeolitic in general) topology represent a class of materials with fascinating structural characteristics and properties,[61–66] these compounds are still the only examples of Zr-MOFs with zeolitic topology.

Herein, we report the templated synthesis of a new 3-dimensional Zr-MOF with the formula $\{[Zr_6(\mu_3\text{-}O)_4(\mu_3\text{-}OH)_4(HCOO)_{12}]_3(Me_2NH_2)_6(4\text{-}MepyH)_6(Cl)_8(CoCl_4)_2\}_n$ – **ZrFA-4**, which represents the third example of a Zr-MOF with the **sod** topology. This compound was formed serendipitously in an attempt to synthesize a heterometallic Zr/Co MOF based on a pyridine-carboxylate ligand and contains a series of guest organic and inorganic, anionic and cationic, species such as $[CoCl_4]^{2-}$, Cl^-, $Me_2NH_2^+$ and 4-$MepyH^+$, which act as templates that direct the formation of a sodalite network. Thus, in this case, the template synthesis enabled the stabilization of a **sod** MOF containing the simplest carboxylate ligands, formate ions, something that has been achieved previously only in one other study by a targeted, cantellation, procedure, employing polytopic ligands with certain geometrical characteristics, designed specifically for this purpose.[61] This compound is also the first example of a 3-dimensional Zr – MOF containing only formate ligands. Gas sorption studies revealed that **ZrFA-4** displays a moderate BET area of 262 $m^2\ g^{-1}$.

Experimental

Materials

Reagent grade chemicals were obtained from commercial sources (Aldrich, Merck, Alfa Aesar, TCI, *etc.*) and used without further purification. All synthetic procedures were carried out in air. 4-((Pyridin-4-ylmethyl)amino)benzoic acid (HINAB) was synthesised following a procedure reported in the literature.[67,68] Other chemical reagents and solvents were of analytical grade and used without further purification.

Synthesis of $\{[Zr_6(\mu_3\text{-}O)_4(\mu_3\text{-}OH)_4(HCOO)_{12}]_3(Me_2NH_2)_6(4\text{-}MepyH)_6(Cl)_8(CoCl_4)_2\}_n$ - ZrFA-4

Solid $ZrCl_4$ (0.023 g, 0.1 mmol) was added in one portion to a clear solution of **HINAB** (0.012 g, 0.05 mmol), $CoCl_2{\cdot}6H_2O$ (0.012 g, 0.05 mmol) and HCOOH (800 μL, 21.20 mmol) in DMF (3 mL) in a 20 mL glass vial and sonicated until complete dissolution of the reactants. The vial was sealed, placed in an oven at 120 °C and left undisturbed for 6 days. Then it was cooled to room temperature and X-ray quality light blue cubic crystals of **ZrFA-4** were isolated by filtration, washed with DMF (3 × 5 mL) and dried in air. The reaction yields were in the range of 15–20% based on $ZrCl_4$. Anal. Calcd.: **ZrFA-4**·5DMF ($Zr_{18}Co_2Cl_{16}O_{101}N_{17}C_{99}H_{179}$), calc.: C 21.42; H 3.25; N 4.29; found: C 21.73; H 3.43; N 4.54.

Physical measurements

Elemental analyses (C, H, N) were performed by the in-house facilities of the University of Cyprus, Chemistry Department. IR spectra were recorded on ATR in the 4000 − 700 cm^{-1} range using a Shimadzu Prestige − 21 spectrometer. pXRD patterns were recorded on a Shimazdu 6000 Series X-ray diffractometer (Cu Kα radiation, λ = 1.5418 Å). Thermal stability studies were performed using a Shimadzu TGA-50 thermogravimetric analyzer in air (flow rate of 10 mL min^{-1}) at a heating rate of 10 °C min^{-1}. Scanning Electron Microscopy (SEM) combined with Energy-Dispersive Spectroscopy (EDS) was carried out using a Thermo Scientific Apreo ChemiSEM System equipped with an integrated EDS detector. ^{1}H NMR spectra were recorded on a Bruker Avance III 300 MHz spectrometer at 25 °C. Chemical shift values in ^{1}H NMR spectra were reported in parts per million (ppm). Digestion of the samples (∼10 mg) was achieved with 0.5 M KOH in D_2O.

Gas adsorption

Low pressure gas sorption measurements were carried out at different temperatures using an Autosorb-iQ3 by Quantachrome system equipped with a cryocooler capable of temperature control from 20 to 320 K. Prior to analysis, the as-synthesized samples were washed with *N*, *N*-dimethylformamide four times per day for 1 day and then soaked in EtOH 3 times per day for 10 days. Finally, the wet samples were transferred to 6 mm sample cells and activated under dynamic vacuum at room temperature for 18 hours until the outgas rate was less than 2 mTorr min^{-1}. After evacuation, the samples were weighed to obtain the precise mass of the evacuated sample, and the cells were transferred to the analysis port of the gas sorption instrument.

Single crystal X-ray crystallography

Single Crystal X-ray diffraction data were collected on a Rigaku Synergy S X-ray diffractometer, equipped with a HyPix-6000HE

area detector utilizing Cu-Ka (λ = 1.5418 Å) radiation. A suitable crystal was mounted on a Hampton cryoloop with Paratone-N oil and transferred to a goniostat, where it was cooled for data collection. The structures were solved by direct methods using SHELXT and OLEX2[69] and refined on F^2 using full-matrix least squares using SHELXL14.1.[70] Software packages used: CrysAlis CCD for data collection, CrysAlis RED for cell refinement and data reduction,[71] and DIAMOND for molecular graphics.[72] The non-H atoms were treated anisotropically, whereas the aromatic hydrogen atoms were placed in calculated, ideal positions and refined as riding on their respective carbon atoms. Hydrogen atoms of the protonated species (μ_3-OH^-, $Me_2NH_2^+$ and 4-$MepyH^+$) were not located in the refined crystal structure. Several restraints (DFIX, DANG, and ISOR) were applied during the refinement to fix the geometry of 4-MepyH, $Me_2NH_2^+$, Cl^- and $[CoCl_4]^{2-}$ ions. Electron density contributions from disordered guest molecules were handled using the SQUEEZE procedure from the PLATON software suit[73] due to their disordered nature. Selected crystal data for **ZrFA-4** are summarized in Table S1 in the SI. CCDC 2536783 contains the supplementary crystallographic data for this paper. Full details can be found in the CIF files provided as SI.

Results and discussion

Synthesis

ZrFA-4 was synthesized serendipitously from a reaction of $ZrCl_4$ and $CoCl_2{\cdot}6H_2O$ with a pyridine carboxylic ligand targeting the isolation of Zr/Co heterometallic MOFs. However, as revealed from the X-ray structure of **ZrFA-4**, the ligand was decomposed under the reaction conditions and its 4-$MepyH^+$ fragment, together with $[CoCl_4]^{2-}$, Cl^- and $Me_2NH_2^+$ acted as templates that enabled the formation of **ZrFA-4**. In particular, the reaction of $ZrCl_4$:$CoCl_2{\cdot}6H_2O$:**HINAB**:HCOOH (**HINAB** = 4-((pyridin-4-ylmethyl)amino)benzoic acid) (Scheme S1, SI) with a molar ratio of 1 : 0.5 : 0.5 : ~200 in DMF (3 mL) at 120 °C for 6 days led to the formation of compound **ZrFA-4**. The MOF was isolated as light blue cubic crystals in ~20% reaction yield. The experimental pXRD pattern of compound **ZrFA-4**, along with the simulated one and the IR spectrum are shown in Fig. S1 and S2 in the SI. Similar reactions to the above one were performed in the absence of $CoCl_2{\cdot}6H_2O$ or/and **HINAB** ligand from the reaction mixture to provide information about the role of the template ions in the formation of **ZrFA-4**. These reactions did not afford **ZrFA-4**, proving that the template ions are essential for its formation. In addition, reactions were performed involving the replacement of $CoCl_2{\cdot}6H_2O$ by other metal salts such as $MnCl_2{\cdot}4H_2O$, which successfully afforded **ZrFA-4** MOF containing $[MnCl_4]^{2-}$ in the place of $[CoCl_4]^{2-}$ ones, as confirmed by a comparison of the pXRD patterns of the reaction product with those of the simulated and experimental **ZrFA-4** (Fig. S3). A comparison of the synthetic procedures that led to the reported Zr-formate complexes revealed that in all cases a large excess of formic acid (for **ZrFA**) or mineral acid (for **ZF-2** and **ZF-3**) is needed to produce the respective compounds. Moreover, the formation of **ZF-3** requires the addition of KNO_3 in the reaction mixture, whereas the synthesis of **ZrFA**, requires, apart from formic acid and a pyridine dicarboxylic acid.[32] These three cases highlight the importance of additives for the synthesis of zirconium-formate phases.[32,34,35] Notably, the formation of **ZrFA-4** requires the use of both a pyridine carboxylic acid ligand (**HINAB**) and a metal ion salt ($CoCl_2{\cdot}6H_2O$) apart from the modulator. This is because the presence of $[CoCl_4]^{2-}$, Cl^- and 4-$MepyH^+$ ions (vide infra) coming from a metal ion salt or an organic ligand added in the reaction mixture and $Me_2NH_2^+$ from the hydrolysis of the solvent (DMF) is necessary for the formation and stabilization of **ZrFA-4**.

The stability of compound **ZrFA-4** treated in various organic solvents was studied with pXRD, which indicated that the compound retains its crystallinity and structural integrity in most organic solvents (Fig. S4). In addition, the thermal stability of **ZrFA-4** was studied with thermogravimetric analysis (Fig. S5). The thermal decomposition of compound **ZrFA-4** proceeds *via* a multi-step process. The first mass losses (until ~330 °C) are attributed to the removal of the lattice DMF molecules and guest template molecules Cl^-/HCl, $Me_2NH_2^+$, 4-$MepyH^+$. The second mass loss, which is completed at 550 °C is attributed to the decomposition of the formate ligand. The residual mass at 900 °C is assigned to zirconium oxide and cobalt oxide.

The morphological features of compound **ZrFA-4** were investigated by field-emission scanning electron microscopy (FESEM). These studies revealed a homogeneous sample containing several well-formed cubic crystals (Fig. S6). Energy-dispersive X-ray spectroscopy (EDS) analysis performed on the blue crystals showed a Zr/Co atomic ratio of ~7, reasonably close to the value expected from single-crystal X-ray crystallography (Zr/Co = 9), considering the semi-quantitative and surface-sensitive nature of the EDS technique.

Description of the structure

Structure elucidation of compound **ZrFA-4** revealed that it crystallizes in the cubic $I\bar{4}3m$ space group. The asymmetric unit of **ZrFA-4** consists of half (Zr1) and one (Zr2) zirconium(IV) cations, one oxo anion, a hydroxide anion, three formate ions (two with full occupancy and two halves), 2/3 chloride anions (one with 50% occupancy and one with 1/6 occupancy), 1/2 $Me_2NH_2^+$, 1/2 4-$MepyH^+$ cations and 1/6 $[CoCl_4]^{2-}$ ions. The structural description of **ZrFA-4** will first focus on the connectivity of the $[Zr_6]$-SBUs that lead to the formation of the sodalite framework (Fig. 1) and then be expanded to the stabilizing organic and inorganic ions that acted as templates enabling the assembly of this structure. All Zr^{4+} ions exhibit the usual tetragonal antiprismatic coordination geometry and occupy the vertices of the octahedral $[Zr_6]$-SBU (Fig. 1a). The coordination sphere of Zr1 ions is completed by two μ_3-O^{2-}, two μ_3-OH^- and four carboxylate O atoms of four $HCOO^-$ anions bridging in the common *syn–syn* (two of them) and *anti–anti* (the remaining two) coordination modes. The coordination sphere of Zr2 ions is completed by two μ_3-O^{2-}, two μ_3-OH^- and four carboxylate O atoms of four $HCOO^-$ anions bridging in the *syn–syn* (three of them) and *anti–anti* (one of them) modes (Fig. 1a). Overall, the coordination sphere of the $[Zr_6(\mu_3\text{-}O)_4(\mu_3\text{-}OH)_4]^{12+}$ structural core of **ZrFA-4** is completed by twelve $HCOO^-$ anions,

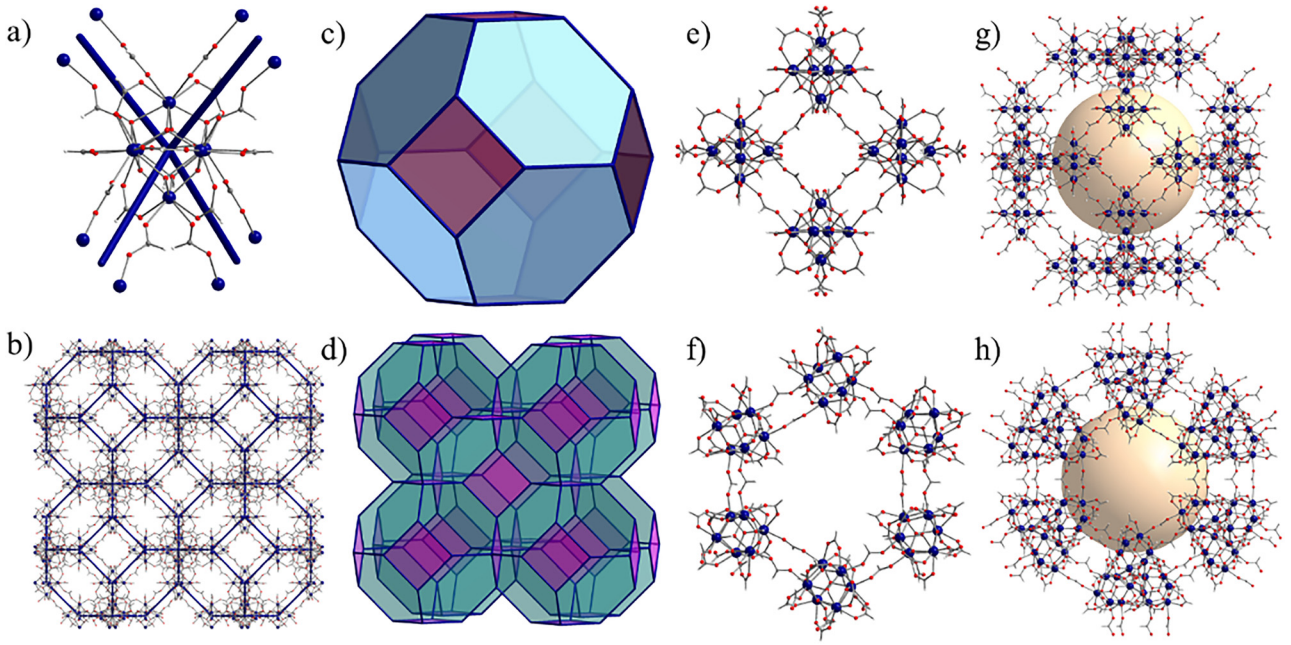

Fig. 1 Representations of the: (a) $[Zr_6(\mu_3\text{-}O^{2-})_4(\mu_3\text{-}OH^-)_4(syn\text{–}syn\text{-}\mu\text{-}HCOO^-)_8(anti\text{–}anti\text{-}\mu\text{-}HCOO^-)_8]^{4-}$ four-coordinated node, with the bold navy-blue lines connecting the centroids of the central $[Zr_6]$ cluster with the centroids of the four neighbouring $[Zr_6]$ clusters; (b) 3-dimensional framework, highlighting the underlying **sod** topology; (c) single truncated octahedral cavity; (d) **sod** network; (e) square and (f) hexagonal apertures; (g) the truncated octahedral cavity emphasizing on the square and (h) the hexagonal apertures of **ZrFA-4**. Colour code: Zr navy blue; O red; C grey; H white.

eight of which (two crystallographically independent with 100% occupancy) bridge two metal ions in the common *syn–syn* mode and four (two crystallographically independent with 50% occupancy) in the *anti–anti* one. The $[Zr_6(\mu_3\text{-}O^{2-})_4(\mu_3\text{-}OH^-)_4(syn\text{–}syn\text{-}\mu\text{-}HCOO^-)_8(anti\text{–}anti\text{-}\mu\text{-}HCOO^-)_4]$ SBU is connected to four neighbouring ones by four pairs of *anti–anti* bridging $HCOO^-$ anions (Fig. 1a and b). Each $[Zr_6]$-SBU is a four-coordinated node giving rise to the formation of a uninodal network with the **sod** topology (Fig. 1c and d). Interestingly, in the structures of sodalite,[74] ZIF-8[64] and Zr-**sod**-ZMOF-1(and -2)[61] the coordination sphere of the metal ions or the extension points of the $[Zr_6]$-SBU is tetrahedral and is completed by four bridging ligands ($\mu\text{-}O^{2-}$, Imidazole and its derivatives) or four triads of dicarboxylate linkers, respectively. In the case of **ZrFA-4** the extension points of the SBU do not form a regular tetrahedron. Instead, the extension points of each four-coordinated $[Zr_6]$-SBU of **ZrFA-4** display two 90° and four 120° angles (Fig. 1a and Fig. S7). This structural feature of **ZrFA-4** highlights the flexibility of this SBU to adopt a variety of conformations depending not only on the linker utilized but also on the template molecules present in the reaction system.[32] To the best of our knowledge, there are three more Zr formate compounds reported in the literature which contain distinctly different structural characteristics than **ZrFA-4**.

A comparison of the crystal structure of **ZrFA-4** with the reported Zr-formate structures **ZrFA**,[32] **ZF-2**,[34] **ZF-3**[34,35] revealed some similarities and also important differences between them, which are summarized in Table 1. Firstly, **ZrFA**, which displays a 2-dimensional structure, exhibits the same square apertures where four $[Zr_6]$ clusters are connected through four pairs of *anti–anti* bridging $HCOO^-$ anions, as is the case for **ZrFA-4** (Fig. 1e and Fig. S8). Moreover, **ZF-2**, **ZF-3**, and **ZrFA-4** display the same hexagonal apertures formed by six $[Zr_6(\mu_3\text{-}O^{2-})_4(\mu_3\text{-}OH^-)_4]^{12+}$

Table 1 Structural comparison of reported Zr-formate compounds (**ZrFA**, **ZF-2**, **ZF-3**) with **ZrFA-4**

Compound	Dimensionality	Polymerization/connectivity	Connection of four $[Zr_6]$ clusters to form square apertures	Connection of six $[Zr_6]$ clusters to form hexagonal apertures	Ref.
ZrFA	2D	2D Layers that are not connected through covalent bonds	Yes (through 4 pairs of *anti–anti* bridging formates between 4 $[Zr_6]$ clusters)	No	32 and 33
ZF-2	0D	Discrete $[Zr_{36}]$ wheel; no covalent connection between $[Zr_6]_6$ hexagons	No	Yes (through 22 $\mu\text{-}O^{2-}$, 6 $\mu\text{-}OH^-$, 4 *anti–anti* $HCOO^-$)	34
ZF-3	3D	$[Zr_6]_6$ hexagons linked through K^+ ions	No	Yes (through 24 $\mu\text{-}O^{2-}/OH^-$, 6 *anti–anti* formates)	34 and 35
ZrFA-4	3D	3D Network (connection of $[Zr_6]_6$ hexagons and $[Zr_6]_4$ squares through *anti–anti* bridging formates)	Yes (through 4 pairs of *anti–anti* bridging formates between 4 $[Zr_6]$ clusters)	Yes (through 12 *anti–anti* bridging formates)	This work

clusters but differ in the way that the hexanuclear clusters are connected to form the hexagons. In particular, each $[Zr_6(\mu_3\text{-}O^{2-})_4(\mu_3\text{-}OH^-)_4]^{12+}$ cluster of the $[Zr_6]_6$ hexagon of **ZrFA-4** is linked to the neighbouring one through a pair of *anti–anti* bridging $HCOO^-$ anions; therefore, the connection of the $[Zr_6]$ units in the $[Zr_6]_6$ hexagon is achieved by 12 *anti–anti* bridging $HCOO^-$ anions in total (Fig. 1f). On the other hand, the $[Zr_6]_6$ hexagons of **ZF-2** and **ZF-3** are formed from the connection of $[Zr_6(\mu_3\text{-}O^{2-})_4(\mu_3\text{-}OH^-)_4]^{12+}$ clusters through twenty-two $\mu\text{-}O^{2-}$, six $\mu\text{-}OH^-$ and four *anti–anti* bridging $HCOO^-$ anions or twenty-four $\mu\text{-}O^{2-}/OH^-$ and six *anti–anti* bridging $HCOO^-$ anions, respectively (Fig. S9). Of course, in **ZF-2**, the $[Zr_6]_6$ hexagons are not connected through covalent bonds with their neighbouring ones and for this reason, this compound is best described as a $[Zr_{36}]$ wheel (0-D material), whereas in **ZF-3**, the $[Zr_6]_6$ hexagons are weakly linked through K^+ cations to form a polymeric species. From this comparison, it is obvious that **ZrFA-4** is the first 3-dimensional Zr-formate MOF where its assembly takes place from the covalent connection of Zr(IV) ions through bridging formate ligands (Fig. S10 and Table 1). **ZrFA-4** is a 3-dimensional framework which features large truncated octahedral cavities with an inner diameter of 20 Å (Fig. 1d, g and h). The solvent accessible volume of **ZrFA-4**, without taking into account the templating ions, was found to be 63% of the unit cell volume.[73]

The assembly of this highly symmetric structure, displaying a very uncommon topology in Zr-MOF chemistry, based on the simplest carboxylate ligands, was very surprising. Several guest organic and inorganic ions which counter-balance each other, since the compound is neutral, were located and refined in the crystal structure of **ZrFA-4**, providing valuable insights on the assembly and stabilization of this MOF structure. For this reason, their presence in the MOF structure and their interactions with the framework of **ZrFA-4** will be discussed in detail. Notably, most of these guest molecules interact with the framework through hydrogen bonds. In particular, 4-methylpyridinium ions (4-MepyH$^+$) formed from the decomposition of **HINAB** molecules under the reaction conditions[75] sit on the top of a pair of *anti–anti* bridging formate ions and interact with them through hydrogen bonds involving the protonated nitrogen atom and the oxygen atoms of the formate ligands (O···N distance: 2.996 Å). Additionally, neighbouring $[Zr_6]$-SBUs are also "bridged" by Cl^- ions which interact through strong hydrogen bonds with two $\mu_3\text{-}OH^-$ on each $[Zr_6]$-SBU (O···Cl distance: 3.050 Å). The Cl^- ions are further immobilized by $Me_2NH_2^+$ ions through weak hydrogen bonds (Cl···N distance: 3.383 Å) (Fig. 2a). A careful examination of the structure reveals that the guest organic and inorganic ions are distributed in both the square and hexagonal apertures. In particular, the former ones feature Cl^- (and $Me_2NH_2^+$ ions) and 4-MepyH$^+$ ions, which are found close to the edges of the $[Zr_6]_4$ square and above and below the plane defined by the centroid of the four $[Zr_6]$-SBUs (Fig. 2b and c). On the other hand, three Cl^- ions and three 4-MepyH$^+$ ions are facing towards the centre of the hexagonal apertures and the remaining 4-MepyH$^+$ ions are located on the periphery of the $[Zr_6]_6$ hexagon, whereas $Me_2NH_2^+$ ions are located within the hexagon. The centre of the hexagonal apertures is occupied by a $[CoCl_4]^{2-}$ ion, which is in close proximity to the

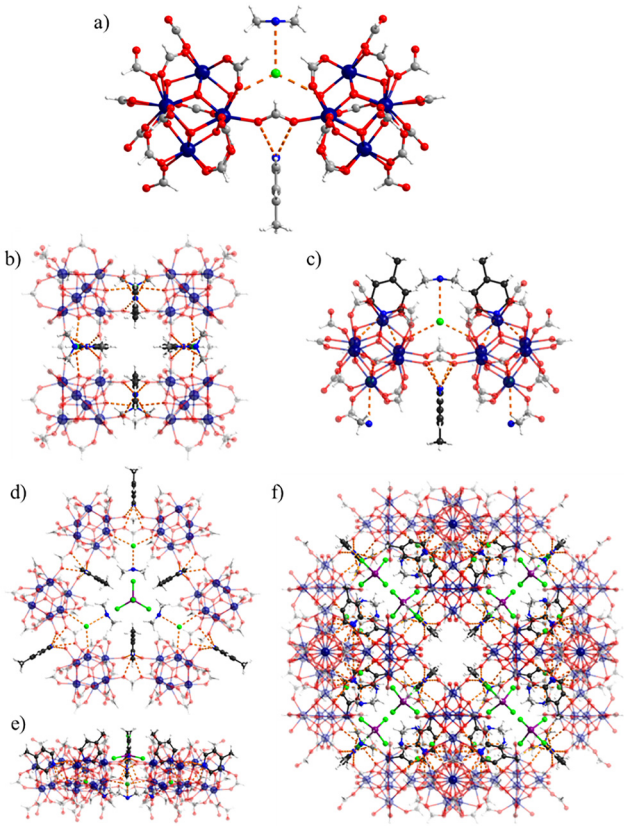

Fig. 2 Representations of the: (a) neighbouring $[Zr_6]$-SBUs interacting with Cl^-, $Me_2NH_2^+$ and 4-MepyH$^+$ ions through H-bonds (orange dashed bonds); (b) front and (c) side view of the square apertures; (d) front and (e) side view of the hexagonal apertures; (f) the sodalite cage including the guest ions of **ZrFA-4**. Colour code: Zr navy blue; Co purple; Cl green; O red; N blue; C grey; (4-MepyH$^+$) black; H white.

4-MepyH$^+$ ions (Fig. 2d and e). Overall, the sodalite cage is stabilized by thirty-two Cl^- ions, twenty-four $Me_2NH_2^+$ ions, twenty-four 4-MepyH$^+$ and eight $[CoCl_4]^{2-}$ ions (Fig. 2f).

Gas sorption properties

Since **ZrFA-4** is stable in low boiling point solvents (Fig. S4) and displays a large solvent accessible volume (excluding guest molecules), we conducted gas adsorption studies. Multiple attempts to activate the material were performed through the exchange of the lattice and coordinated solvent molecules with various low boiling point solvents. One of the goals was the removal of the guest organic and inorganic molecules/ions without decomposition of the structure. These attempts possibly enabled the successful removal of some of the guest molecules, as evidenced by the change in crystal colour from light blue to colourless during the exchange process (Fig. S11). This colour change may be attributed to the removal of $[CoCl_4]^{2-}$, although modifications in the coordination sphere/number of the Co^{2+} ions upon treatment with EtOH could also account for the observed colour change. In addition, ^{1}H-NMR studies revealed that the guest molecules were not removed completely from the pores of **ZrFA-4** (Fig. S12). Attempts to remove all the guest

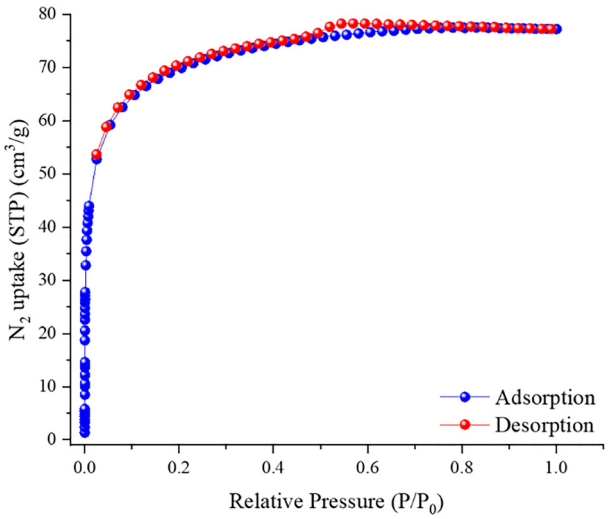

Fig. 3 Low pressure N_2 adsorption isotherm of **ZrFA-4** at 77 K.

molecules from the structure by exchange with additional solvents or/and under intense conditions (exchange at high temperatures or by employing the Soxhlet extraction process) led to partial and in some cases complete collapse of the structure. The optimum activation of **ZrFA-4** was achieved after treatment with EtOH (Fig. S4). N_2 sorption measurements at 77 K of **ZrFA-4**, activated with EtOH, revealed a type-I isotherm typical for microporous solids (Fig. 3), from which the apparent BET area was determined to 262 $m^2\ g^{-1}$ (Langmuir, 305 $m^2\ g^{-1}$) (Fig. S13 and S14). The total pore volume value of 0.12 $cm^3\ g^{-1}$ at relative pressure, $p/p_0 = 0.99$, is lower compared to the value of 0.62 $cm^3\ g^{-1}$ calculated for the completely evacuated structure of **ZrFA-4**.

The lower surface area and pore volume values obtained for **ZrFA-4** are attributed to the trapped organic/inorganic molecules in the pores of the compound and/or partial collapse of the framework (Fig. S12). The pore size distribution was calculated using non-local density functional theory (NLDFT) after a successful fitting of the N_2 adsorption isotherm data using a suitable NLDFT kernel (Fig. S15). The pore size distribution of **ZrFA-4** shows a major peak centred at ~9.7 Å, which can be rationalized based on the crystal structure when the templating ions are included. Minor peaks are also observed at 22.7 Å, which can be rationalized by considering the activated structure after removal of the templating ions. An additional peak at 30.9 Å cannot be rationalized based on the crystallographic data and is therefore attributed to partial collapse of the framework (Fig. S16). The CO_2 uptake was investigated up to 1 bar at 273 K, 283 K and 298 K (Fig. S17). **ZrFA-4** was found to adsorb 1.9 (8.4 wt%), 1.4 (6.1 wt%) and 0.9 (3.8 wt%) mmol $CO_2\ g^{-1}$ and the isosteric heat of adsorption, Q_{st}^0, was calculated to 32 kJ mol^{-1} (Fig. S18 and S19). These results are in line with the findings for the other Zr-formate compounds, which are either non-porous (**ZF-2** and **ZF-3**)[34,35] or exhibit moderate porosity and CO_2 uptake, as in the case of **ZrFA** (BET surface area of ~136 $m^2\ g^{-1}$ and CO_2 adsorption capacity of 1.44 mmol g^{-1} at 293 K and 1100 mbar).[32,33]

Conclusions

In summary, a new Zr-formate phase was serendipitously discovered by investigating reactions targeting the synthesis of heterometallic Zr/Co-MOFs. **ZrFA-4** represents the third example of a Zr-MOF with the **sod** topology and a zeolite-like topology in general, the first 3-dimensional Zr-formate MOF and a rare example of a Zr-MOF with only formate ligands reported. Interestingly, the only other examples of Zr **sod**-MOFs reported previously were synthesized using pre-designed polytopic ligands with certain geometrical characteristics, selected specifically for this purpose. Thus, the stabilization of a structure exhibiting a very unusual topology in Zr-MOF chemistry, based on the simplest carboxylic ligands, was quite surprising and achieved because of the template process that took place under the reaction conditions. The templating ions were located and refined in the structure of **ZrFA-4**, revealing a series of interactions with the framework that are responsible for the formation and stabilization of this structure. The N_2 adsorption isotherm of **ZrFA-4** revealed a moderate specific BET surface area of 262 $m^2\ g^{-1}$, whereas the CO_2 sorption studies an uptake of 1.9 (8.4 wt%) mmol $CO_2\ g^{-1}$ at 273 K and a Q_{st}^0, of 32 kJ mol^{-1}. Overall, this work emphasizes the capability of template synthesis to stabilize unique MOF structures and provides insights into the role of small organic and inorganic molecules in the formation and stabilization of extended framework structures.

Author contributions

Laoura Komodiki: investigation, methodology, and writing original draft. Nikos Panagiotou: investigation, methodology, project supervision and writing original draft. Giannis S. Papaefstathiou: investigation, methodology, writing original draft, reviewing and editing. Anastasios J. Tasiopoulos: project supervision and manuscript writing, reviewing and editing.

Data availability

All data supporting the findings of this study are included within the article and its supplementary information (SI). The SI contains crystallographic data, synthetic procedures, PXRD patterns, IR spectra, thermogravimetric analysis (TGA), SEM images, structural representations, NMR spectra and gas sorption measurements for **ZrFA-4**. See DOI: https://doi.org/10.1039/d6ma00342g.

Further details can be obtained from the corresponding author upon request.

CCDC 2536783 contains the supplementary crystallographic data for this paper.[76]

Conflicts of interest

There are no conflicts to declare.

Acknowledgements

This work was funded by the project, entitled "Integrated Approaches at Local Scale for Enhancing Water Reuse

Efficiency and Sustainable Soil Fertilization from Wastewater's Recovered Nutrients'', acronym ''CIRQUA'', Grant agreement No. 2321, Call 2023 Section 1 Management of Water IA, which is part of the PRIMA programme supported by the European Union.

Notes and references

1 D. J. Tranchemontagne, J. L. Mendoza-Cortés, M. O'Keeffe and O. M. Yaghi, Secondary building units, nets and bonding in the chemistry of metal-organic frameworks, *Chem. Soc. Rev.*, 2009, **38**, 1257.
2 G. Férey, Hybrid porous solids: Past, present, future, *Chem. Soc. Rev.*, 2008, **37**, 191.
3 M. Eddaoudi, D. F. Sava, J. F. Eubank, K. Adil and V. Guillerm, Zeolite-like metal-organic frameworks (ZMOFs): Design, synthesis, and properties, *Chem. Soc. Rev.*, 2015, **44**, 228.
4 J. Zhao, X. Liu, Y. Wu, D.-S. Li and Q. Zhang, Surfactants as promising media in the field of metal-organic frameworks, *Coord. Chem. Rev.*, 2019, **391**, 30.
5 H. Furukawa, K. E. Cordova, M. O'Keeffe and O. M. Yaghi, The chemistry and applications of metal-organic frameworks, *Science*, 2013, **341**, 1230444, DOI: 10.1126/science.1230444.
6 J. Guo, S. Chu, F. Yuan, K. Otake, M.-S. Yao and S. Kitagawa, Soft porous crystals: flexible MOFs as a new class of adaptive materials, *Ind. Chem. Mater.*, 2025, **3**, 651.
7 A. Kumar, D. G. Madden, M. Lusi, K.-J. Chen, E. A. Daniels, T. Curtin, J. J. Perry IV and M. J. Zaworotko, Direct Air Capture of CO_2 by Physisorbent Materials, *Angew. Chem., Int. Ed.*, 2015, **54**, 14372.
8 B. Li, H.-M. M. Wen, W. Zhou, J. Q. Q. Xu and B. Chen, Porous Metal-Organic Frameworks: Promising Materials for Methane Storage, *Chem*, 2016, **1**, 557.
9 X. Zhao, Y. Wang, D.-S. Li, X. Bu and P. Feng, Metal–Organic Frameworks for Separation, *Adv. Mater.*, 2018, **30**, 1705189.
10 J. S. Ravishan Fernando and S. M. Chavan, Bio-based mixed linker of zirconium MOFs and the beads for CO_2 separation, *Sep. Purif. Technol.*, 2025, **378**, 134675.
11 S. Krause, N. Hosono and S. Kitagawa, Chemistry of Soft Porous Crystals: Structural Dynamics and Gas Adsorption Properties, *Angew. Chem., Int. Ed.*, 2020, **59**, 15325.
12 M. Gehre, Z. Guo, G. Rothenberg and S. Tanase, Sustainable Separations of C_4-Hydrocarbons by Using Microporous Materials, *ChemSusChem*, 2017, **10**, 3947.
13 S. L. Anderson, P. G. Boyd, A. Gładysiak, T. N. Nguyen, R. G. Palgrave, D. Kubicki, L. Emsley, D. Bradshaw, M. J. Rosseinsky, B. Smit and K. C. Stylianou, Nucleobase pairing and photodimerization in a biologically derived metal-organic framework nanoreactor, *Nat. Commun.*, 2019, **10**, 1612.
14 A. Dhakshinamoorthy, Z. Li and H. Garcia, Catalysis and photocatalysis by metal organic frameworks, *Chem. Soc. Rev.*, 2018, **47**, 8134.
15 M. Zhao, S. Huang, Q. Fu, W. Li, R. Guo, Q. Yao, F. Wang, P. Cui, C. H. Tung and D. Sun, Ambient Chemical Fixation of CO_2 Using a Robust Ag_{27} Cluster-Based Two-Dimensional Metal–Organic Framework, *Angew. Chem., Int. Ed.*, 2020, **59**, 20031.
16 H. Wang, W. P. Lustig and J. Li, Sensing and capture of toxic and hazardous gases and vapors by metal-organic frameworks, *Chem. Soc. Rev.*, 2018, **47**, 4729.
17 E. A. Dolgopolova, A. M. Rice, C. R. Martin and N. B. Shustova, Photochemistry and photophysics of MOFs: Steps towards MOF-based sensing enhancements, *Chem. Soc. Rev.*, 2018, **47**, 4710.
18 W. M. Chen, X. L. Meng, G. L. Zhuang, Z. Wang, M. Kurmoo, Q. Q. Zhao, X. P. Wang, B. Shan, C. H. Tung and D. Sun, A superior fluorescent sensor for Al^{3+} and UO_2^{2+} based on a Co(II) metal-organic framework with exposed pyrimidyl Lewis base sites, *J. Mater. Chem. A*, 2017, **5**, 13079.
19 A. E. Psalti, S. V. Eliseeva, A. Hatzidimitriou, S. Oikonomidis, S. Petoud and T. Lazarides, Luminescent Lanthanide Metal–Organic Frameworks for Temperature Sensing in Two Distinct Temperature Regions, *J. Am. Chem. Soc.*, 2026, **148**, 4020.
20 S. A. Diamantis, A. Margariti, A. D. Pournara, G. S. Papaefstathiou, M. J. Manos and T. Lazarides, Luminescent metal-organic frameworks as chemical sensors: Common pitfalls and proposed best practices, *Inorg. Chem. Front.*, 2018, **5**, 1493.
21 Y. Gao, P. Jing, N. Yan, M. Hilbers, H. Zhang, G. Rothenberg and S. Tanase, Dual-mode humidity detection using a lanthanide-based metal-organic framework: towards multifunctional humidity sensors, *Chem. Commun.*, 2017, **53**, 4465.
22 J. Li, X. X. Wang, G. Zhao, C. Chen, Z. Chai, A. Alsaedi, T. Hayat and X. X. Wang, Metal-organic framework-based materials: Superior adsorbents for the capture of toxic and radioactive metal ions, *Chem. Soc. Rev.*, 2018, **47**, 2322.
23 P. A. Kobielska, A. J. Howarth, O. K. Farha and S. Nayak, Metal–organic frameworks for heavy metal removal from water, *Coord. Chem. Rev.*, 2018, **358**, 92.
24 M. Feng, P. Zhang, H.-C. Zhou and V. K. Sharma, Water-stable metal-organic frameworks for aqueous removal of heavy metals and radionuclides: A review, *Chemosphere*, 2018, **209**, 783.
25 P. Kumar, A. Pournara, K.-H. H. Kim, V. Bansal, S. Rapti and M. J. Manos, Metal-organic frameworks: Challenges and opportunities for ion-exchange/sorption applications, *Prog. Mater. Sci.*, 2017, **86**, 25.
26 S. Rathod, S. Bercha, M. B. Yagci, D. Yilmaz, O. Zavorotynska and S. M. Chavan, Thiol functionalized metal–organic framework for efficient silver adsorption and removal from aqueous solution, *J. Mater. Chem. A*, 2025, **13**, 39785.
27 D. A. Evangelou, E. C. Makri, N. Pliatsios, I. Vamvasakis, E. Buchsteiner, P. Oikonomopoulos, G. S. Armatas, G. S. Papaefstathiou, T. Lazarides and M. J. Manos, Ultramicroporous Al(III) MOFs with selective CO_2 adsorption, acid resistance, and efficient Cr(VI) sorption properties, *Dalton. Trans.*, 2025, **54**, 13658.
28 S. Yuan, L. Feng, K. Wang, J. Pang, M. Bosch, C. Lollar, Y. Sun, J. Qin, X. Yang, P. Zhang, Q. Wang, L. Zou, Y. Zhang, L. Zhang, Y. Fang, J. Li and H. C. Zhou, Stable Metal–Organic Frameworks: Design, Synthesis, and Applications, *Adv. Mater.*, 2018, **30**, 1.

29 J. H. Cavka, S. Jakobsen, U. Olsbye, N. Guillou, C. Lamberti, S. Bordiga and K. P. Lillerud, A new zirconium inorganic building brick forming metal organic frameworks with exceptional stability, *J. Am. Chem. Soc.*, 2008, **130**, 13850.

30 Y. Bai, Y. Dou, L. H. Xie, W. Rutledge, J. R. Li and H. C. Zhou, Zr-based metal-organic frameworks: Design, synthesis, structure, and applications, *Chem. Soc. Rev.*, 2016, **45**, 2327.

31 G. K. Angeli, D. Batzavali, K. Mavronasou, C. Tsangarakis, T. Stuerzer, H. Ott and P. N. Trikalitis, Remarkable Structural Diversity between Zr/Hf and Rare-Earth MOFs via Ligand Functionalization and the Discovery of Unique (4, 8)-c and (4, 12)-connected Frameworks, *J. Am. Chem. Soc.*, 2020, **142**, 15986.

32 W. Liang, R. Babarao, M. J. Murphy and D. M. D'Alessandro, The first example of a zirconium-oxide based metal-organic framework constructed from monocarboxylate ligands, *Dalton Trans.*, 2015, **44**, 1516.

33 X. H. Xiong, L. Song, W. Wang, X. Y. Zhu, L. L. Meng, H. T. Zheng, Z. W. Wei, L. L. Tan, X. C. Huang and C. Y. Su, Synthesis and Modification of Formate Zr-MOF (ZrFA) Toward Scalable and Cost-Cutting Gas Separation, *Angew. Chem., Int. Ed.*, 2025, **64**, e202505978.

34 J. I. Choi, H. Chun and M. S. Lah, Zirconium-Formate Macrocycles and Supercage: Molecular Packing versus MOF-like Network for Water Vapor Sorption, *J. Am. Chem. Soc.*, 2018, **140**, 10915.

35 M. Wahiduzzaman, S. Nandi, V. Yadav, K. Taksande, G. Maurin, H. Chun and S. Devautour-Vinot, Superionic conduction in a zirconium-formate molecular solid, *J. Mater. Chem. A*, 2020, **8**, 17951.

36 Z. Chen, S. L. Hanna, L. R. Redfern, D. Alezi, T. Islamoglu and O. K. Farha, Reticular chemistry in the rational synthesis of functional zirconium cluster-based MOFs, *Coord. Chem. Rev.*, 2019, **386**, 32.

37 A. M. Tollitt, R. Vismara, L. M. Daniels, D. Antypov, M. W. Gaultois, A. P. Katsoulidis and M. J. Rosseinsky, High-Throughput Discovery of a Rhombohedral Twelve-Connected Zirconium-Based Metal-Organic Framework with Ordered Terephthalate and Fumarate Linkers, *Angew. Chem., Int. Ed.*, 2021, **60**, 26939.

38 C. Zou, S. Vagin, A. Kronast and B. Rieger, Template mediated and solvent-free route to a variety of UiO-66 metal–organic frameworks, *RSC Adv.*, 2016, **6**, 102968.

39 M. J. Manos, E. E. Moushi, G. S. Papaefstathiou and A. J. Tasiopoulos, New Zn^{2+} metal organic frameworks with unique network topologies from the combination of trimesic acid and amino-alcohols, *Cryst. Growth Des.*, 2012, **12**, 5471.

40 E. E. Moushi, A. Kourtellaris, E. Andreou, A. Fidelli, G. S. Papaefstathiou, J. C. Plakatouras and A. J. Tasiopoulos, New metal-organic frameworks derived from pyridine-3,5-dicarboxylic acid: Structural diversity arising from the addition of templates into the reaction systems, *CrystEngComm*, 2020, **22**, 2083.

41 I. Mylonas-Margaritis, J. Mayans, W. Tong, P. Farràs, A. Escuer, P. McArdle and C. Papatriantafyllopoulou, Synthesis and characterization of new coordination compounds by the use of 2-pyridinemethanol and di- or tricarboxylic acids, *CrystEngComm*, 2021, **23**, 5489.

42 C. Paraschiv, A. Cucos, S. Shova, A. M. Madalan, C. Maxim, D. Visinescu, B. Cojocaru, V. I. Parvulescu and M. Andruh, New Zn(II) coordination polymers constructed from amino-alcohols and aromatic dicarboxylic acids: Synthesis, structure, photocatalytic properties, and solid-state conversion to ZnO, *Cryst. Growth Des.*, 2015, **15**, 799.

43 J. P. Vizuet, M. L. Mortensen, A. L. Lewis, M. A. Wunch, H. R. Firouzi, G. T. McCandless and K. J. Balkus, Fluoro-Bridged Clusters in Rare-Earth Metal-Organic Frameworks, *J. Am. Chem. Soc.*, 2021, **143**, 17995.

44 F. Dimakopoulou, C. G. Efthymiou, A. Kourtellaris, C. O'Malley, L. Alaa Eldin Refat, A. Tasiopoulos, P. McArdle and C. Papatriantafyllopoulou, Synthesis and characterisation of new coordination polymers by combining 2-pyridyl oximes or alcohols with functionalised terephthalic acid analogues, *CrystEngComm*, 2023, **25**, 6080.

45 N. Zhao, K. Cai and H. He, The synthesis of metal–organic frameworks with template strategies, *Dalton Trans.*, 2020, **49**, 11467.

46 X. Guo, S. Geng, M. Zhuo, Y. Chen, M. J. Zaworotko, P. Cheng and Z. Zhang, The utility of the template effect in metal-organic frameworks, *Coord. Chem. Rev.*, 2019, **391**, 44.

47 M. Eddaoudi, D. B. Moler, H. Li, B. Chen, T. M. Reineke, M. O'Keeffe and O. M. Yaghi, Modular chemistry: Secondary building units as a basis for the design of highly porous and robust metal-organic carboxylate frameworks, *Acc. Chem. Res.*, 2001, **34**, 319.

48 X. Tang, L. Jia, X. Wang, S. Su, Y. Chen, X. Kong, Z. Ye, H. Xie, W. Gong, E. Du, Y. Liu, K. O. Kirlikovali, O. K. Farha and Y. Cui, The Last Piece of the Puzzle: Access to 7-Connected Zirconium Metal–Organic Frameworks for Hexane Separation, *Angew. Chem.*, 2025, **64**, e202424859.

49 A. Dhakshinamoorthy, A. M. Asiri and H. Garcia, Mixed-metal or mixed-linker metal organic frameworks as heterogeneous catalysts, *Catal. Sci. Technol.*, 2016, **6**, 5238.

50 M. Y. Masoomi, A. Morsali, A. Dhakshinamoorthy and H. Garcia, Mixed-Metal MOFs: Unique Opportunities in Metal–Organic Framework (MOF) Functionality and Design, *Angew. Chem.*, 2019, **131**, 15330.

51 T. N. Tu, M. V. Nguyen, H. L. Nguyen, B. Yuliarto, K. E. Cordova and S. Demir, Designing bipyridine-functionalized zirconium metal–organic frameworks as a platform for clean energy and other emerging applications, *Coord. Chem. Rev.*, 2018, **364**, 33.

52 M. I. Gonzalez, E. D. Bloch, J. A. Mason, S. J. Teat and J. R. Long, Single-crystal-to-single-crystal metalation of a metal-organic framework: A route toward structurally well-defined catalysts, *Inorg. Chem.*, 2015, **54**, 2995.

53 K. Manna, T. Zhang, F. X. Greene and W. Lin, Bipyridine- and Phenanthroline-Based Metal–Organic Frameworks for Highly Efficient and Tandem Catalytic Organic Transformations via Directed C–H Activation, *J. Am. Chem. Soc.*, 2015, **137**, 2665.

54 T. Kajiwara, M. Fujii, M. Tsujimoto, K. Kobayashi, M. Higuchi, K. Tanaka and S. Kitagawa, Photochemical Reduction of Low Concentrations of CO_2 in a Porous Coordination Polymer with a Ruthenium(II)–CO Complex, *Angew. Chem., Int. Ed.*, 2016, **55**, 2697.

55 C. Wang, Z. Xie, K. E. DeKrafft and W. Lin, Doping Metal–Organic Frameworks for Water Oxidation, Carbon Dioxide Reduction, and Organic Photocatalysis, *J. Am. Chem. Soc.*, 2011, **133**, 13445.
56 M. I. Gonzalez, A. B. Turkiewicz, L. E. Darago, J. Oktawiec, K. Bustillo, F. Grandjean, G. J. Long and J. R. Long, Confinement of atomically defined metal halide sheets in a metal–organic framework, *Nature*, 2020, **577**, 64.
57 S. Yuan, J. S. Qin, J. Su, B. Li, J. Li, W. Chen, H. F. Drake, P. Zhang, D. Yuan, J. Zuo and H. C. Zhou, Sequential Transformation of Zirconium(IV)-MOFs into Heterobimetallic MOFs Bearing Magnetic Anisotropic Cobalt(II) Centers, *Angew. Chem., Int. Ed.*, 2018, **57**, 12578.
58 Y. Zhou and B. Yan, Ratiometric detection of temperature using responsive dual-emissive MOF hybrids, *J. Mater. Chem. C*, 2015, **3**, 9353.
59 G. Nickerl, M. Leistner, S. Helten, V. Bon, I. Senkovska and S. Kaskel, Integration of accessible secondary metal sites into MOFs for H_2S removal, *Inorg. Chem. Front.*, 2014, **1**, 325.
60 W. A. Maza, A. J. Haring, S. R. Ahrenholtz, C. C. Epley, S. Y. Lin and A. J. Morris, Ruthenium(II)-polypyridyl zirconium(IV) metal-organic frameworks as a new class of sensitized solar cells, *Chem. Sci.*, 2016, **7**, 719.
61 N. Alsadun, G. Mouchaham, V. Guillerm, J. Czaban-Jóźwiak, A. Shkurenko, H. Jiang, P. M. Bhatt, P. Parvatkar and M. Eddaoudi, Introducing a Cantellation Strategy for the Design of Mesoporous Zeolite-like Metal–Organic Frameworks: Zr-sod-ZMOFs as a Case Study, *J. Am. Chem. Soc.*, 2020, **142**, 20547.
62 H. Wang, L. Han, D. Zheng, M. Yang, Y. H. Andaloussi, P. Cheng, Z. Zhang, S. Ma, M. J. Zaworotko, Y. Feng and Y. Chen, Protein-Structure-Directed Metal–Organic Zeolite-like Networks as Biomacromolecule Carriers, *Angew. Chem., Int. Ed.*, 2020, **59**, 6263.
63 T. He, X.-J. Kong, J. Zhou, C. Zhao, K. Wang, X.-Q. Wu, X.-L. Lv, G.-R. Si, J.-R. Li and Z.-R. Nie, A Practice of Reticular Chemistry: Construction of a Robust Mesoporous Palladium Metal–Organic Framework via Metal Metathesis, *J. Am. Chem. Soc.*, 2021, **143**, 9901.
64 K. S. Park, Z. Ni, A. P. Côté, J. Y. Choi, R. Huang, F. J. Uribe-Romo, H. K. Chae, M. O'Keeffe, O. M. Yaghi, M. O'Keeffe and O. M. Yaghi, Exceptional chemical and thermal stability of zeolitic imidazolate frameworks, *Proc. Natl. Acad. Sci. U. S. A.*, 2006, **103**, 10186.
65 C. M. McGuirk, T. Runčevski, J. Oktawiec, A. Turkiewicz, M. K. Taylor and J. R. Long, Influence of Metal Substitution on the Pressure-Induced Phase Change in Flexible Zeolitic Imidazolate Frameworks, *J. Am. Chem. Soc.*, 2018, **140**, 15924.
66 M. Asgari, R. Semino, P. A. Schouwink, I. Kochetygov, J. Tarver, O. Trukhina, R. Krishna, C. M. Brown, M. Ceriotti and W. L. Queen, Understanding How Ligand Functionalization Influences CO_2 and N_2 Adsorption in a Sodalite Metal-Organic Framework, *Chem. Mater.*, 2020, **32**, 1526.
67 W.-Y. Wong and W.-T. Wong, Synthesis, structural characterization and solvatochromic studies of a series of Schiff base-containing triosmium alkylidyne carbonyl clusters, *J. Organomet. Chem.*, 1999, **584**, 48.
68 S. Abedi, A. Azhdari Tehrani, H. Ghasempour and A. Morsali, Interplay between hydrophobicity and basicity toward the catalytic activity of isoreticular MOF organocatalysts, *New J. Chem.*, 2016, **40**, 6970.
69 O. V. Dolomanov, A. J. Blake, N. R. Champness and M. Schröder, OLEX: New software for visualization and analysis of extended crystal structures, *J. Appl. Crystallogr.*, 2003, **36**, 1283.
70 G. M. Sheldrick, A short history of SHELX, *Acta Cryst.*, 2008, **64**, 112.
71 E. OxfordDiffraction, CrysAlis CCD and CrysAlis RED, version p171.38.46; Oxford Diffraction Ltd, Abingdon, Oxford, 2017.
72 K. Brandenburg, *Diamond, Version 3.2k*, 2014.
73 A. L. Spek, Single-crystal structure validation with the program PLATON, *J. Appl. Crystallogr.*, 2003, **36**, 7.
74 I. Hassan and H. D. Grundy, The crystal structures of sodalite-group minerals, *Acta Crystallogr., Sect. B: Struct. Sci.*, 1984, **40**, 6.
75 A. K. Singh, S. Jang, J. Y. Kim, S. Sharma, K. C. Basavaraju, M. G. Kim, K. R. Kim, J. S. Lee, H. H. Lee and D. P. Kim, One-Pot Defunctionalization of Lignin-Derived Compounds by Dual-Functional $Pd_{50}Ag_{50}/Fe_3O_4$/N-rGO Catalyst, *ACS Catal.*, 2015, **5**, 6964.
76 CCDC 2536783: Experimental Crystal Structure Determination, 2026, DOI: 10.5517/ccdc.csd.cc2r4qqc.